

# **Non-empirical semilocal functionals for improved performance in quantum chemistry and materials science**

**E. Fabiano**

NNL – Nanoscience Institute of CNR  
Lecce, Italy

## INTRODUCTION

- Semilocal exchange-correlation functionals
- The family of PBE-like XC functionals

## GGA functionals

- PBEint
- zPBEint
- APBE
- Q2D-GGA

## Meta-GGA functionals

- TPSSloc

## INTRODUCTION

- Semilocal exchange-correlation functionals
- The family of PBE-like XC functionals

## GGA functionals

- PBEint
- zPBEint
- APBE
- Q2D-GGA

## Meta-GGA functionals

- TPSSloc

Kohn-Sham (KS) density functional theory is at present one of the most powerful computational tools in quantum chemistry and materials science

$$\left[ -\frac{1}{2}\nabla^2 + v_{ext}(\mathbf{r}) + \int \frac{\rho(\mathbf{r}')}{|\mathbf{r} - \mathbf{r}'|} d\mathbf{r}' + v_{xc}(\mathbf{r}) \right] \psi_i(\mathbf{r}) = \epsilon_i \psi_i(\mathbf{r}) \quad \text{KS equations}$$

A main ingredient in this scheme is the exchange-correlation (XC) energy functional and its various approximations

$$v_{xc}(\mathbf{r}) = \frac{\delta E_{xc}[\rho]}{\delta \rho(\mathbf{r})}$$

The development of more efficient XC functionals has been, and still is, one the main research topic in DFT

Kohn-Sham (KS) density functional theory is at present one of the most powerful computational tools in quantum chemistry and materials science

$$\left[ -\frac{1}{2}\nabla^2 + v_{ext}(\mathbf{r}) + \int \frac{\rho(\mathbf{r}')}{|\mathbf{r} - \mathbf{r}'|} d\mathbf{r}' + v_{xc}(\mathbf{r}) \right] \psi_i(\mathbf{r}) = \epsilon_i \psi_i(\mathbf{r}) \quad \text{KS equations}$$

A main ingredient in this scheme is the exchange-correlation (XC) energy functional and its various approximations

$$v_{xc}(\mathbf{r}) = \frac{\delta E_{xc}[\rho]}{\delta \rho(\mathbf{r})} \quad \text{The development of more efficient XC functionals has been, and still is, one the main research topic in DFT}$$

Nowadays several accurate approaches exist to approximate the XC functional, including exact exchange and perturbative correlation expansions.

Nevertheless, **in practical applications semilocal functionals, depending only on the electron density and its derivatives, are generally preferred due to their favorable cost-to-accuracy ratio**

$$E_{xc}^{GGA} \approx \int \epsilon_{xc}^{GGA}(\rho, \nabla \rho) d\mathbf{r} = \int \epsilon_{xc}^{LDA} F(\rho, |\nabla \rho|^2) d\mathbf{r} \quad \text{Generalized gradient approximations}$$

$$E_{xc}^{mGGA} \approx \int \epsilon_{xc}^{mGGA}(\rho, \nabla \rho, \tau) d\mathbf{r} \quad \tau = \frac{1}{2} \sum_i^{\text{occ.}} |\nabla \psi_i|^2 \quad \text{Meta-generalized gradient approximations}$$

# The PBE family of exchange-correlation functionals

## PBE functional form

**exchange:**  $E_x[\rho_\uparrow, \rho_\downarrow] = \frac{E_x[2\rho_\uparrow] + E_x[2\rho_\downarrow]}{2}$

$$E_x[\rho] = \int \rho \epsilon^{\text{unif}}(\rho) F_x(s) d\mathbf{r}$$

$$F_x(s) = 1 + \kappa - \frac{\kappa}{1 + (\mu/\kappa)s^2}$$

## correlation:

$$E_c^{PBE}[\rho_\uparrow, \rho_\downarrow] = \int \rho [\epsilon_c^{\text{unif}}(r_s, \zeta) + H(r_s, \zeta, t)] d\mathbf{r}$$

$$H(r_s, \zeta, t) = \gamma \phi^3 \ln \left( 1 + \frac{\beta}{\gamma} \frac{t^2 + At^4}{1 + At^2 + A^2 t^4} \right)$$

J.P. Perdew, K. Burke, M. Ernzerhof, Phys. Rev. Lett. **77**, 3865 (1996)

# The PBE family of exchange-correlation functionals



## PBE functional form

**exchange:**  $E_x[\rho_\uparrow, \rho_\downarrow] = \frac{E_x[2\rho_\uparrow] + E_x[2\rho_\downarrow]}{2}$

$$E_x[\rho] = \int \rho \epsilon^{\text{unif}}(\rho) F_x(s) d\mathbf{r}$$
$$F_x(s) = 1 + \kappa - \frac{\kappa}{1 + (\mu/\kappa)s^2}$$

## correlation:

$$E_c^{PBE}[\rho_\uparrow, \rho_\downarrow] = \int \rho [\epsilon_c^{\text{unif}}(r_s, \zeta) + H(r_s, \zeta, t)] d\mathbf{r}$$
$$H(r_s, \zeta, t) = \gamma \phi^3 \ln \left( 1 + \frac{\beta}{\gamma} \frac{t^2 + At^4}{1 + At^2 + A^2 t^4} \right)$$

J.P. Perdew, K. Burke, M. Ernzerhof, Phys. Rev. Lett. **77**, 3865 (1996)

Several variants of the PBE XC functional have been developed, playing with  $(\mu, \kappa, \beta)$  parameters

## Physically motivated:

- **PBEsol**: restoring the second-order gradient expansion for exchange

$$(\mu^{\text{GE2}}=10/81, \kappa^{\text{PBE}}=0.804, \beta=0.046)$$

J.P. Perdew et al., Phys. Rev. Lett. **77**, 3865 (1996)

- **PBEmol**: Self-interaction in H atom

$$(\mu=0.276, \kappa^{\text{PBE}}=0.804, \beta=3\mu/\pi^2)$$

J. M. del Campo et al., J. Chem. Phys. **136**, 104108 (2012)

## Semiempirical:

- **revPBE**: fit to exchange energy of atoms  
( $\mu^{\text{PBE}}=0.21951, \kappa^{\text{revPBE}}=1.245, \beta=0.066725$ )

Y. Zhang, W. Yang, Phys. Rev. Lett. **80**, 890 (1998)

- **xPBE**: fit to atomic and molecular data  
( $\mu=0.23214, \kappa=0.91954, \beta=0.089809$ )

X. Xu, W.A. Goddard, J. Chem. Phys. **121**, 4068 (2004)

## INTRODUCTION

- Semilocal exchange-correlation functionals
- The family of PBE-like XC functionals

## GGA functionals

- **PBEint**
- zPBEint
- APBE
- Q2D-GGA

## Meta-GGA functionals

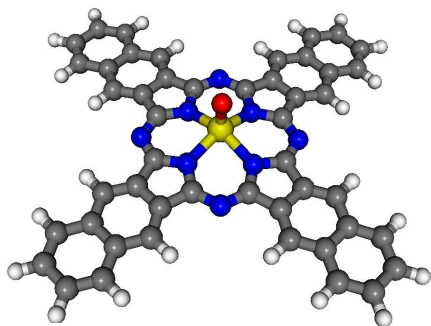
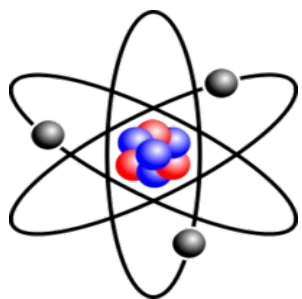
- TPSSloc



# The PBEint functional

## PBE functional

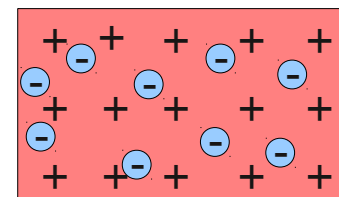
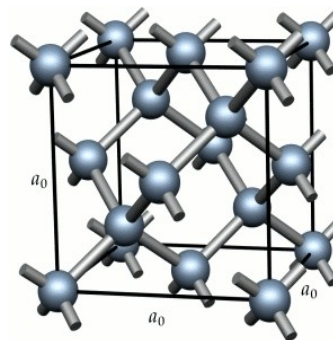
rapidly varying density regime:



$$\begin{aligned}\mu &= \mu^{\text{PBE}} = 0.21951 \\ \kappa &= 0.804 \quad \beta = 0.066725\end{aligned}$$

## PBEsol functional

slowly varying density regime:

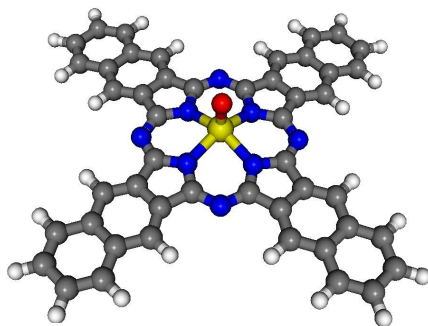
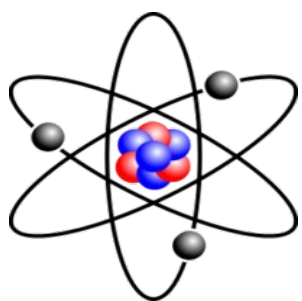


$$\begin{aligned}\mu &= \mu^{\text{GE2}} = 10/81 \\ \kappa &= 0.804 \quad \beta = 0.046\end{aligned}$$

# The PBEint functional

## PBE functional

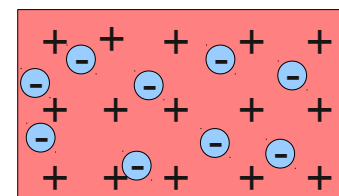
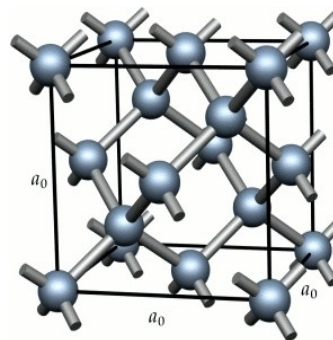
rapidly varying density regime:



$$\mu = \mu^{\text{PBE}} = 0.21951$$
$$\kappa = 0.804 \quad \beta = 0.066725$$

## PBEsol functional

slowly varying density regime:



$$\mu = \mu^{\text{GE2}} = 10/81$$
$$\kappa = 0.804 \quad \beta = 0.046$$

None of them works for intermediate density regimes, e.g. hybrid interfaces or metal clusters

## PBEint functional

Modifies the PBE exchange enhancement factor to interpolate between the rapidly- and slowly-varying density regimes

$$\alpha = \frac{(\mu^{\text{GE2}})^2}{\kappa(\mu^{\text{PBE}} - \mu^{\text{GE2}})} = 0.197 \longrightarrow \text{smooth derivative}$$

$$\kappa = 0.804 \longrightarrow \text{Local Lieb-Oxford bound}$$

$$\beta = 0.052 \longrightarrow \text{exact hole-constraint on jellium correlation surface energies}$$

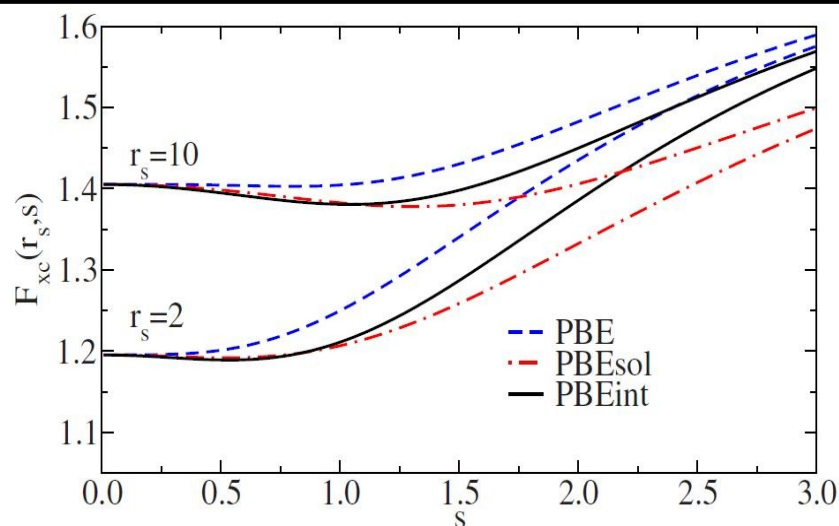
$$\mu(s) = \mu^{\text{GE2}} + \frac{(\mu^{\text{PBE}} - \mu^{\text{GE2}})\alpha s^2}{1 + \alpha s^2}$$

works for molecules and solids

accurate for intermediate

and/or mixed density regimes

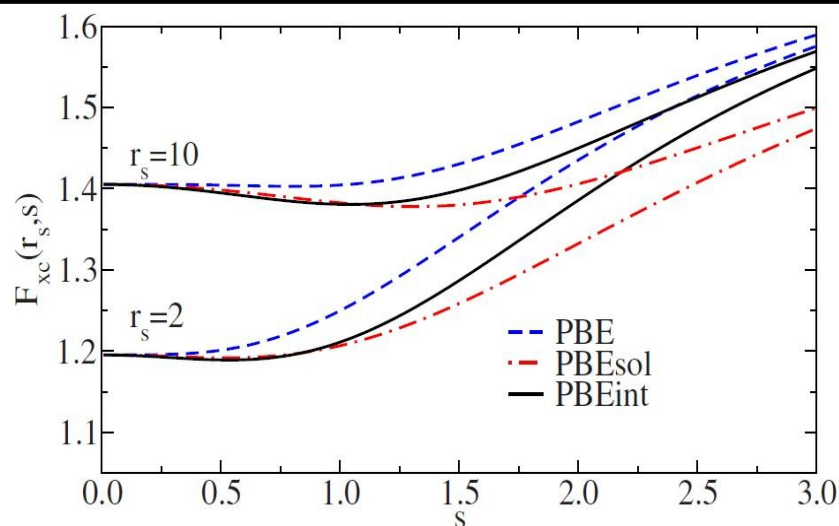
# Assessment of the PBEint functional



The PBEint XC enhancement factor effectively interpolates between PBE and PBEsol, favoring a **balanced description of both the rapidly- and slowly-varying density regimes** and reducing error cancellation between X and C for interfaces

E. Fabiano, L.A. Constantin, F. Della Sala, Phys. Rev. B **82**, 113104 (2010)  
E. Fabiano, L.A. Constantin, F. Della Sala, J. Chem. Theory Comput. **7**, 3548 (2011)  
E. Fabiano, L.A. Constantin, F. Della Sala, J. Chem. Phys. **134**, 194112 (2011)  
L.A. Constantin, L. Chiodo, E. Fabiano, I. Bodrenko, F. Della Sala, Phys. Rev. B **84**, 045126 (2011)

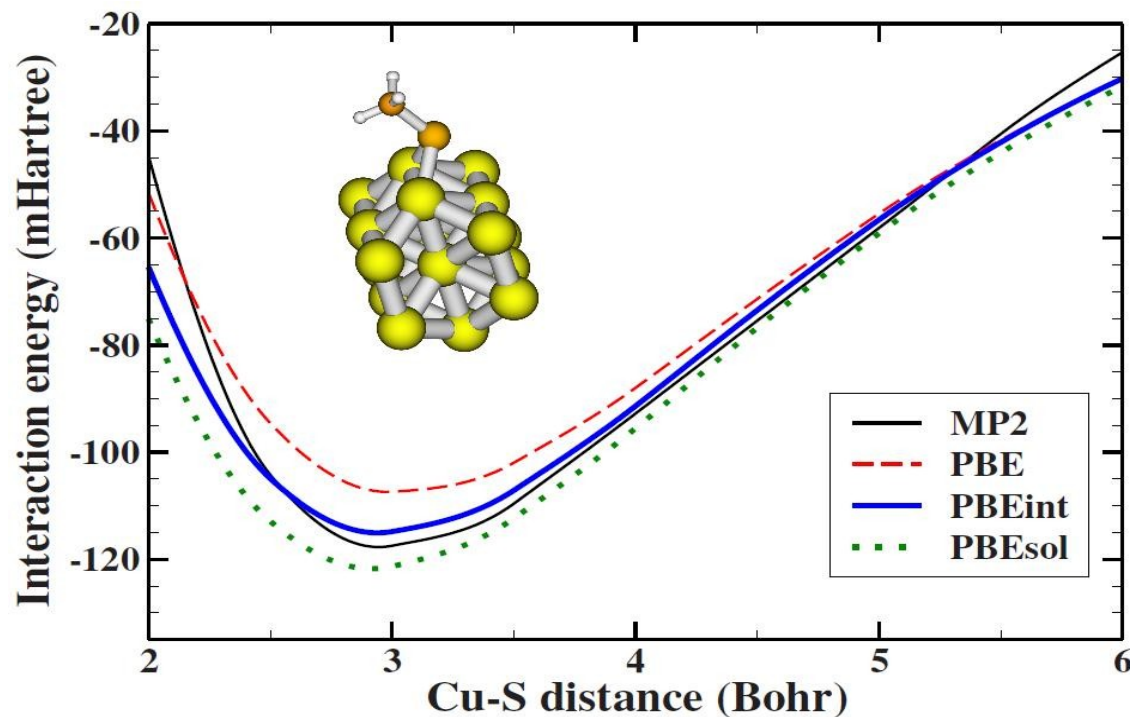
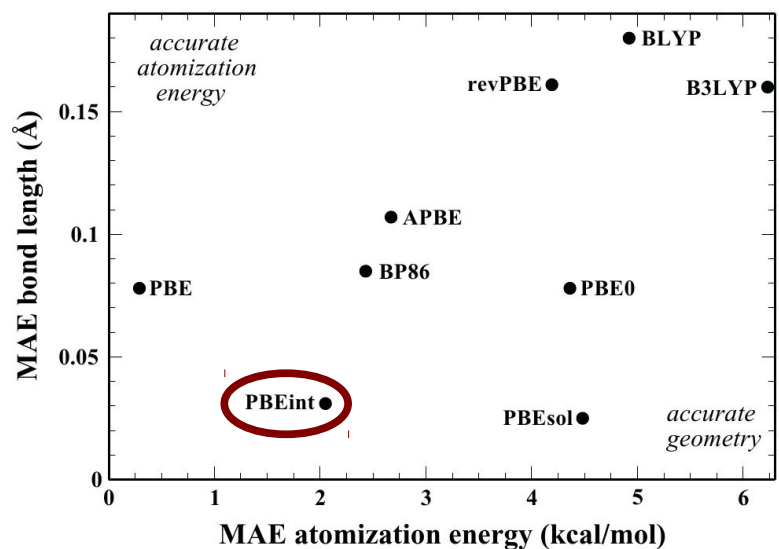
# Assessment of the PBEint functional



Because of its ability to correctly describe different density regimes, the PBEint functional is especially accurate for:

- surfaces and interfaces
- hybrid metal-molecule interfaces
- metal clusters
- cohesive energies of solids

The PBEint XC enhancement factor effectively interpolates between PBE and PBEsol, favoring a **balanced description of both the rapidly- and slowly-varying density regimes** and reducing error cancellation between X and C for interfaces



E. Fabiano, L.A. Constantin, F. Della Sala, Phys. Rev. B **82**, 113104 (2010)  
 E. Fabiano, L.A. Constantin, F. Della Sala, J. Chem. Theory Comput. **7**, 3548 (2011)  
 E. Fabiano, L.A. Constantin, F. Della Sala, J. Chem. Phys. **134**, 194112 (2011)  
 L.A. Constantin, L. Chiodo, E. Fabiano, I. Bodrenko, F. Della Sala, Phys. Rev. B **84**, 045126 (2011)

## INTRODUCTION

- Semilocal exchange-correlation functionals
- The family of PBE-like XC functionals

## GGA functionals

- PBEint
- **zPBEint**
- APBE
- Q2D-GGA

## Meta-GGA functionals

- TPSSloc

# Spin-dependent correlation correction

The PBEint functional performs very well for clusters and interfaces, but shows a limited accuracy for atomization energies of molecular systems.

This problem can be mostly overcome by considering a **spin-dependent correction for the correlation** energy, in order to have a better balance in the description of different systems.

$$\epsilon_{xc} = \epsilon_x^{LDA} F_x(s) + \epsilon_c^{LDA} + f(\phi, t) H^{PBE}$$

For the spin-dependent correction-factor two different ansatzes were considered:

## z-corrected functionals

$$f(\phi, t) = \phi^{\alpha t^3} \quad \phi = \frac{(1 + \zeta)^{2/3} + (1 - \zeta)^{2/3}}{2}$$

L.A. Constantin, E. Fabiano, F. Della Sala, Phys. Rev. B **84**, 233103 (2011)

## zv-corrected functionals

$$f(\zeta, v) = e^{-\alpha v^3 |\zeta|^\omega} \quad v = \frac{|\nabla \rho|}{2 \left( \frac{3}{4\pi^4} \right)^{1/18} \rho^{10/9}}$$

L.A. Constantin, E. Fabiano, F. Della Sala, J. Chem. Phys., submitted

## Properties:

- The two ansatzes are identical at small and large spin-polarizations
- For a slowly-varying density,  $f \rightarrow 1$  (the correct slowly-varying density limit of GGAs is preserved)
- For  $\zeta \rightarrow 0$ ,  $f \rightarrow 1$  (no correction when no spin polarization)
- zv-ansatz: the spatial and spin behaviors can be tuned independently



# 1e-density model systems

The parameter  $\alpha$  and the density parameter  $v$  in the spin-dependent correction term can be fixed by considering a statistical ensemble of the one-electron density models

$$\rho^H(r) = \frac{e^{-2r}}{\pi} ; \rho^G(r) = \frac{e^{-r^2}}{\pi^{3/2}} ; \rho^C(r) = \frac{(1+r)e^{-r}}{32\pi}$$

The optimal value of the parameters is obtained by minimization of the information-entropy-like function

$$I = - \sum_i p_i R_i \ln(p_i R_i) \quad i = H, G, C$$

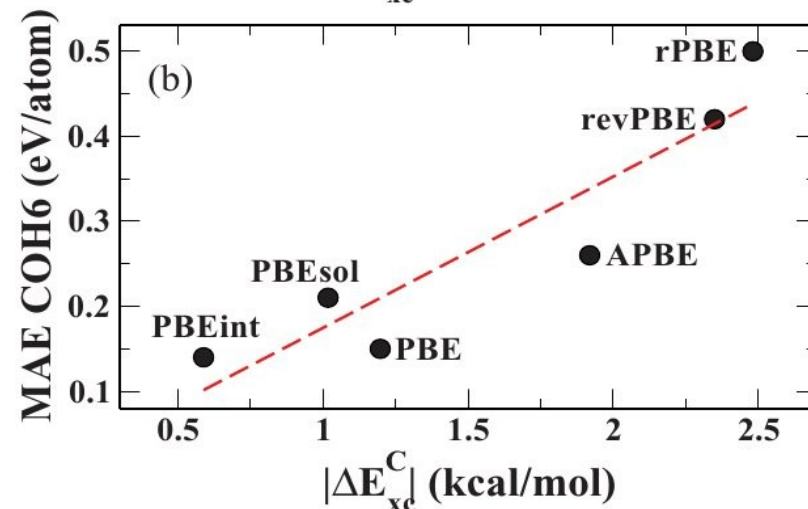
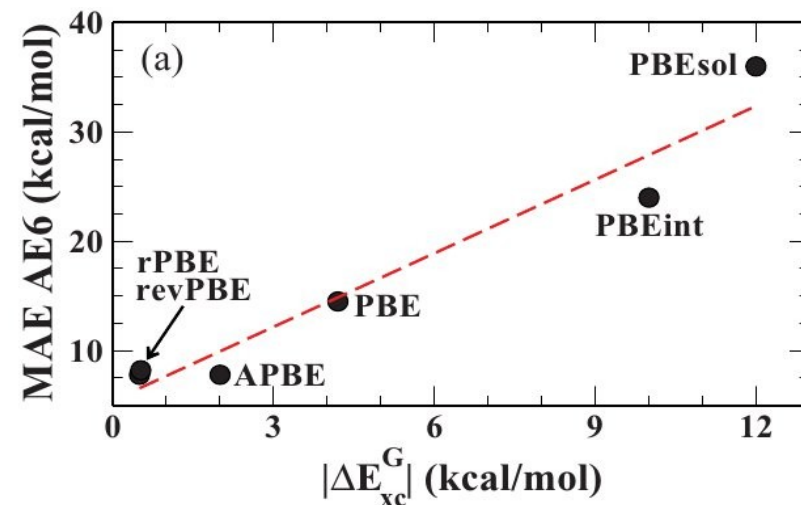
with

$$p_i = 1/3 \quad (\text{equ-probability assumption})$$

$$R_i = \left| \Delta E_{xc}^i / E_x^{exact} \right|$$

L.A. Constantin, E. Fabiano, F. Della Sala, Phys. Rev. B **84**, 233103 (2011)

L.A. Constantin, E. Fabiano, F. Della Sala, J. Chem. Phys., submitted



# Partially polarized Gaussian model densities

The parameter  $\omega$  the zv-spin-dependent correction can be fixed by considering the uniformly partially-polarized one-electron Gaussian densities

$$\rho_{\uparrow} = \frac{1 + \zeta}{2} \frac{e^{-r^2}}{\pi^{3/2}} ; \rho_{\downarrow} = \frac{1 - \zeta}{2} \frac{e^{-r^2}}{\pi^{3/2}}$$

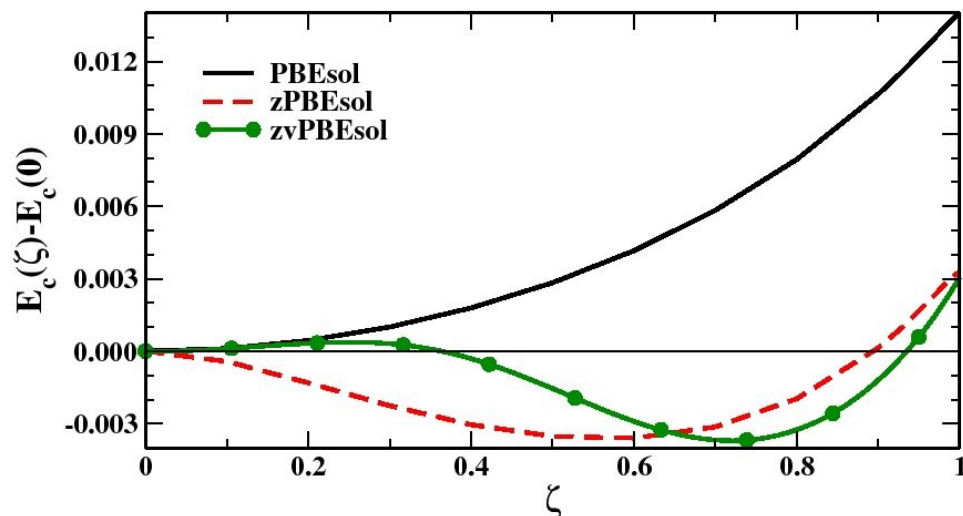
The parameter  $\omega$  is fixed by imposing the following conditions:

The correction shall vanish in the core region and only act in valence and tail regions, which are relevant for bonding

$$\left. \frac{dE_c^{zv-GGA}}{d\zeta} \right|_{\zeta \leq 0.3} \approx 0$$

The two ansatzes must be equal in the valence and tail regions

$$\left. \frac{d(E_c^{zv-GGA} - E_c^{z-GGA})}{d\zeta} \right|_{\zeta \geq 0.7} \approx 0$$



	zPBEint	zPBEsol	zvPBEint	zvPBEsol
$\alpha$	2.4	4.8	1.0	1.6
$\omega$	-	-	4.5	4.5



# Assessment of the z- and zv-corrected functionals

We tested the z- and zv-corrected functionals for several binding and cohesive properties as well as for different properties of spin-polarized systems

Test	units	PBEsol	zPBEsol	zvPBEsol	PBEint	zPBEint	zvPBEint	PBE
Atomization and binding energies								
AE6 (organic molecules)	kcal/mol	34.90	15.72	<b>14.21</b>	24.78	14.62	<b>14.06</b>	14.50
W4 (organic molecules)	kcal/mol	21.45	<b>12.64</b>	13.72	15.57	<b>11.59</b>	12.32	10.75
TM10AE (transition metals)	kcal/mol	18.29	10.70	<b>9.24</b>	15.58	10.63	<b>8.50</b>	13.47
AUnAE (gold clusters)	kcal/mol	4.37	<b>1.97</b>	2.43	2.22	1.01	<b>0.85</b>	0.31
SI7 (hybrid interfaces)	kcal/mol	3.92	<b>2.88</b>	3.28	2.80	2.72	<b>2.50</b>	3.69
Other properties								
BL9 (organic molecules)	mÅ	<b>15</b>	16	<b>15</b>	17	<b>15</b>	16	15
TM10BL (transition metals)	mÅ	19	<b>17</b>	18	18	<b>17</b>	<b>17</b>	23
K9 (kinetics)	kcal/mol	10.83	<b>9.90</b>	10.42	9.17	<b>8.73</b>	9.03	7.51
$\Delta E_S$ (spin states)	%	102	<b>74</b>	87	90	<b>72</b>	81	79

Note that for the spin-unpolarized case the z- and zv-corrected functionals recover the results of the original PBEint (PBEsol) functional, so they are very accurate for many important properties (lattice constants of paramagnetic solids, bond lengths of closed-shell molecules, metal clusters, interfaces,...)

L.A. Constantin, E. Fabiano, F. Della Sala, Phys. Rev. B **84**, 233103 (2011)

L.A. Constantin, E. Fabiano, F. Della Sala, J. Chem. Phys., submitted

## INTRODUCTION

- Semilocal exchange-correlation functionals
- The family of PBE-like XC functionals

## GGA functionals

- PBEint
- zPBEint
- **APBE**
- Q2D-GGA

## Meta-GGA functionals

- TPSSloc

# Semiclassical atom model system



For many-electron neutral atoms the kinetic and exchange energy are given with good accuracy (asymptotically exact) by the semiclassical formulas

$$T_s \approx c_0 Z^{7/3} + c_1 Z^2 + c_2 Z^{5/3} + \dots$$

$$E_x \approx E_x^{LDA} + d_1 Z + d_2 Z^{2/3} + \dots$$

The zeroth-order term of the semiclassical expansions is recovered by the local density and Thomas-Fermi approximations.

The higher-order corrections are due to higher-order quantum effects.

For many-electron neutral atoms the kinetic and exchange energy are given with good accuracy (asymptotically exact) by the semiclassical formulas

$$T_s \approx c_0 Z^{7/3} + c_1 Z^2 + c_2 Z^{5/3} + \dots$$

$$E_x \approx E_x^{LDA} + d_1 Z + d_2 Z^{2/3} + \dots$$

The zeroth-order term of the semiclassical expansions is recovered by the local density and Thomas-Fermi approximations.

The higher-order corrections are due to higher-order quantum effects.

The ordinary second-order gradient expansions

$$T_s \approx \int \tau_s^{TF} (1 + \mu_s s^2) d\mathbf{r}, \quad \mu_s = 5/27$$

$$E_x \approx \int \epsilon_x^{LDA} (1 + \mu_x s^2) d\mathbf{r}, \quad \mu_x = 10/81$$

cannot reproduce the leading corrections in the semiclassical expansions.

However, **the  $c_1$  and  $d_1$  coefficients are very well reproduced by considering a modified second-order gradient expansion** with

$$\mu_s^{\text{MGE2}} = 0.23889, \quad \mu_x^{\text{MGE2}} = 0.26$$

The coefficients from the modified second-order gradient expansion can be used into a generalized gradient approximation to obtain density functionals able to reproduce (in the slowly-varying density limit) the semiclassical expansions for atoms.

The APBE functional is constructed by considering a PBE-like functional form within the semiclassical atom model.

The exchange enhancement factor uses the parameters

$$\mu = \mu_x^{\text{MGE2}} = 0.26 \quad ; \quad \kappa = 0.804$$

The correlation coefficient is fixed by imposing the LDA linear response condition

$$\beta = 3\mu_x^{\text{MGE2}} / \pi^2 \approx 0.079$$

The APBE functional contains **no empirical parameters** and respects most of the exact constraint of the PBE functional.

By construction, it **recovers the modified second-order gradient expansion for exchange** and thus the **semiclassical limit for many-electron neutral atoms**.

# Assessment of the APBE functional



Test set	PBE	APBE	revPBE	BLYP
Atomization energies (kcal/mol)				
Organic molecules	<u>14.50</u>	7.98	8.85	<b>6.85</b>
Metal complexes	<u>10.52</u>	7.39	<b>6.33</b>	9.02
Transition metals	6.26	<b>6.05</b>	<u>7.85</u>	6.64
Overall MAE	<u>10.95</u>	<b>7.28</b>	7.66	7.61
Bond lengths (mÅ)				
Organic molecules	<b>9.27</b>	9.44	11.44	<u>12.34</u>
Metal complexes	9.19	<b>8.24</b>	<u>16.51</u>	15.63
Transition metals	<b>52.8</b>	57.3	<u>62.2</u>	57.2
Overall MAE <sup>a</sup>	8.70	<b>8.68</b>	11.77	<u>12.11</u>
Solid-state systems				
Lattice constants (mÅ)	<b>71</b>	90	130	<u>151</u>
Bulk moduli (GPa)	<b>10.3</b>	15.0	15.8	<u>23.1</u>
Surface XC energy (erg/cm <sup>2</sup> )	<b>42</b>	50	62	<u>279</u>

The APBE functional outperforms PBE (as well as other GGAs) for molecular systems for both atomization energies and bond lengths.

For solid-state systems it is reasonably close to PBE and better than other GGA functionals specialized for molecules.

L.A. Constantin, E. Fabiano, S. Laricchia, F. Della Sala,  
Phys. Rev. Lett. **106**, 186406 (2011)

E. Fabiano, L. A. Constantin, F. Della Sala,  
J. Chem. Theory Comput. **7**, 3548 (2011)

# Assessment of the APBE functional

Test set	PBE	APBE	revPBE	BLYP
Atomization energies (kcal/mol)				
Organic molecules	<u>14.50</u>	7.98	8.85	<b>6.85</b>
Metal complexes	<u>10.52</u>	7.39	<b>6.33</b>	9.02
Transition metals	6.26	<b>6.05</b>	<u>7.85</u>	6.64
Overall MAE	<u>10.95</u>	<b>7.28</b>	7.66	7.61
Bond lengths (mÅ)				
Organic molecules	<b>9.27</b>	9.44	11.44	<u>12.34</u>
Metal complexes	9.19	<b>8.24</b>	<u>16.51</u>	15.63
Transition metals	<b>52.8</b>	57.3	<u>62.2</u>	57.2
Overall MAE <sup>a</sup>	8.70	<b>8.68</b>	11.77	<u>12.11</u>
Solid-state systems				
Lattice constants (mÅ)	<b>71</b>	90	130	<u>151</u>
Bulk moduli (GPa)	<b>10.3</b>	15.0	15.8	<u>23.1</u>
Surface XC energy (erg/cm <sup>2</sup> )	<b>42</b>	50	62	<u>279</u>

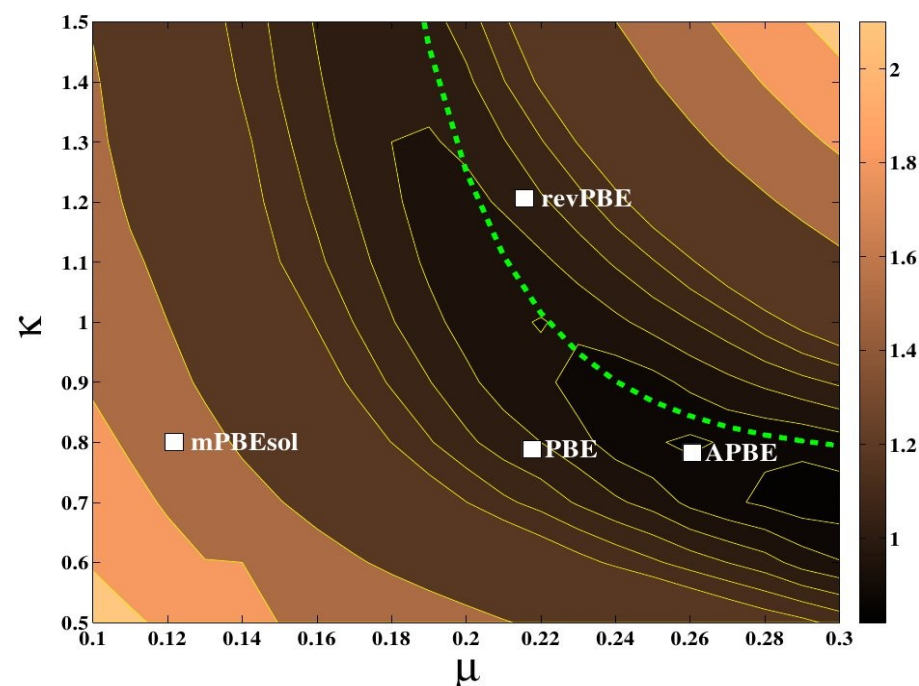
The APBE functional outperforms PBE (as well as other GGAs) for molecular systems for both atomization energies and bond lengths.

For solid-state systems it is reasonably close to PBE and better than other GGA functionals specialized for molecules.

**The parameters defining the APBE functional correspond, for molecular properties, almost to an absolute minimum of the accuracy among all the functionals belonging to the PBE family**

L.A. Constantin, E. Fabiano, S. Laricchia, F. Della Sala, Phys. Rev. Lett. **106**, 186406 (2011)

E. Fabiano, L. A. Constantin, F. Della Sala, J. Chem. Theory Comput. **7**, 3548 (2011)





# Overall performance



Test	units	PBE	PBEsol	PBEint	zPBEint	APBE
Organic molecules						
Atomiz. energy (AE6)	kcal/mol	14.5	34.9	24.7	14.6	<b>7.9</b>
Atomiz. energy (W4)	kcal/mol	10.7	21.5	15.5	11.6	<b>8.5</b>
Reaction energy (OMRE)	kcal/mol	6.8	12.0	8.2	<b>6.5</b>	7.1
Reaction energy (DC9)	kcal/mol	<b>10.6</b>	17.6	15.5	14.8	12.1
Barrier heights	kcal/mol	9.5	13.1	11.4	9.7	<b>8.3</b>
Kinetics (K9)	kcal/mol	7.5	10.6	9.1	8.7	<b>6.6</b>
Bond lengths	mÅ	<b>9</b>	10	10	10	<b>9</b>
Vib. frequencies	cm <sup>-1</sup>	56.8	65.9	65.4	65.2	<b>55.0</b>
Transition-metal complexes						
Atomiz. energy	kcal/mol	13.4	18.3	15.5	10.6	<b>8.7</b>
Reaction energy	kcal/mol	3.7	9.9	6.9	6.5	<b>3.1</b>
Bond lengths	mÅ	12	22	16	15	<b>11</b>
Clusters and interfaces						
Cluster atom. en.	kcal/mol	<b>0.3</b>	4.4	2.2	1.0	1.7
Cluster bond lengths	mÅ	90	<b>29</b>	42	41	125
Small interfaces	kcal/mol	3.7	3.9	2.8	<b>2.7</b>	5.8
Non-bonded interactions						
Hydrogen bond	kcal/mol	0.4	1.7	0.5	0.5	<b>0.3</b>
Dipole-dipole	kcal/mol	<b>0.4</b>	1.0	<b>0.4</b>	<b>0.4</b>	<b>0.4</b>
CT complexes	kcal/mol	2.7	4.1	3.0	3.0	<b>2.3</b>
Solid state						
Cohesive energy	eV	0.15	0.21	<b>0.14</b>	0.16	0.26
Lattice const.	mÅ	59	<b>22</b>	32	32	79

The APBE functional provides very accurate results for molecular systems (both organic and transition-metal complexes) and is **one of the best methods for non-bonded interactions**

E. Fabiano, L.A. Constantin, F. Della Sala, Phys. Rev. B **82**, 113104 (2010)

E. Fabiano, L.A. Constantin, F. Della Sala, J. Chem. Theory Comput. **7**, 3548 (2011)

E. Fabiano, L.A. Constantin, F. Della Sala, J. Chem. Phys. **134**, 194112 (2011)

L.A. Constantin, E. Fabiano, S. Laricchia, F. Della Sala, Phys. Rev. Lett. **106**, 186406 (2011)

L.A. Constantin, E. Fabiano, F. Della Sala, Phys. Rev. B **84**, 233103 (2011)



## INTRODUCTION

- Semilocal exchange-correlation functionals
- The family of PBE-like XC functionals

## GGA functionals

- PBEint
- zPBEint
- APBE
- **Q2D-GGA**

## Meta-GGA functionals

- TPSSloc

## 3D to 2D dimensional crossover



The 3D to 2D dimensional crossover is related to the one-dimensional nonuniform scaling of the density

$$\rho_{\sigma\lambda}^z = \lambda \rho_{\sigma}(x, y, \lambda z) \quad \lambda \rightarrow \infty$$

Under this scaling the exchange and correlation energies per particle must respect

$$0 > \lim_{\lambda \rightarrow \infty} \epsilon_x[\rho_{\uparrow\lambda}^z, \rho_{\downarrow\lambda}^z] > -\infty$$

$$0 \geq \lim_{\lambda \rightarrow \infty} \epsilon_c[\rho_{\uparrow\lambda}^z, \rho_{\downarrow\lambda}^z] > -\infty$$

**However, popular XC approximations do not respect these limits!!**

## 3D to 2D dimensional crossover

The 3D to 2D dimensional crossover is related to the one-dimensional nonuniform scaling of the density

$$\rho_{\sigma\lambda}^z = \lambda \rho_{\sigma}(x, y, \lambda z) \quad \lambda \rightarrow \infty$$

Under this scaling the exchange and correlation energies per particle must respect

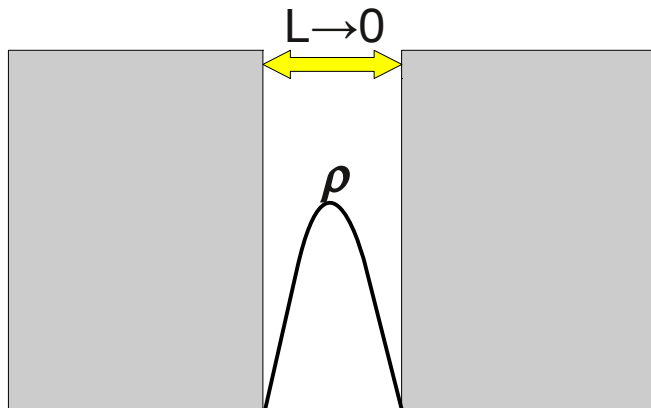
$$0 > \lim_{\lambda \rightarrow \infty} \epsilon_x[\rho_{\uparrow\lambda}^z, \rho_{\downarrow\lambda}^z] > -\infty$$

$$0 \geq \lim_{\lambda \rightarrow \infty} \epsilon_c[\rho_{\uparrow\lambda}^z, \rho_{\downarrow\lambda}^z] > -\infty$$

**However, popular XC approximations do not respect these limits!!**

### Infinite-barrier model

The 2D limit can be modeled by considering an one-dimensional infinite-barrier quantum well of thickness  $L$ , with  $L \rightarrow 0$  and the 2D electron-density ( $\rho^{2D}$ ) kept constant



$$\Psi_{l,\mathbf{k}_{\parallel}}(\mathbf{r}_{\parallel}, z) = \sqrt{\frac{2}{AL}} \sin\left(\frac{l\pi z}{L}\right) e^{i\mathbf{r}_{\parallel} \cdot \mathbf{k}_{\parallel}} \quad 0 \leq z \leq L$$

$$E_{l,\mathbf{k}_{\parallel}} = \frac{1}{2} \left[ \left(\frac{l\pi}{L}\right)^2 + \mathbf{k}_{\parallel}^2 \right] \quad L \leq \sqrt{\frac{3\pi}{2\rho^{2D}}}$$

# The Q2D-GGA functional

Because the quasi-2D regions are characterized by a rapidly-varying density regime, an XC functional capable to describe the 3D to 2D crossover in solids can be constructed by interpolating between the 3D limit (at slowly-varying densities) and the 2D limit (at rapidly-varying densities)

$$\epsilon_x^{Q2D} = \frac{\epsilon_x^{PBEsol} (a - s^4) + b \epsilon_x^{LDA} s^{7/2} (1 + s^2)}{a + s^6}$$

$$\epsilon_c^{Q2D} = \epsilon_c^{PBE} + \frac{t^4 (1 + t^2)}{c + t^6} [\epsilon_c^{2D-LDA} - \epsilon_c^{PBE}]$$

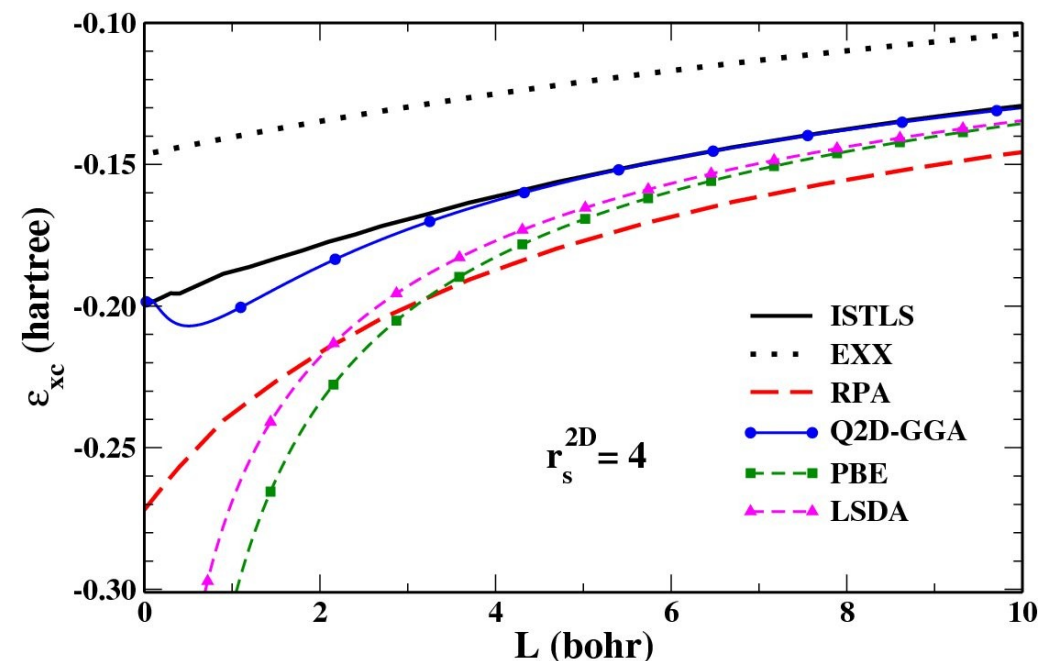
The parameters

$$a = 10^2$$

$$b = 0.5217$$

$$c = 10^6$$

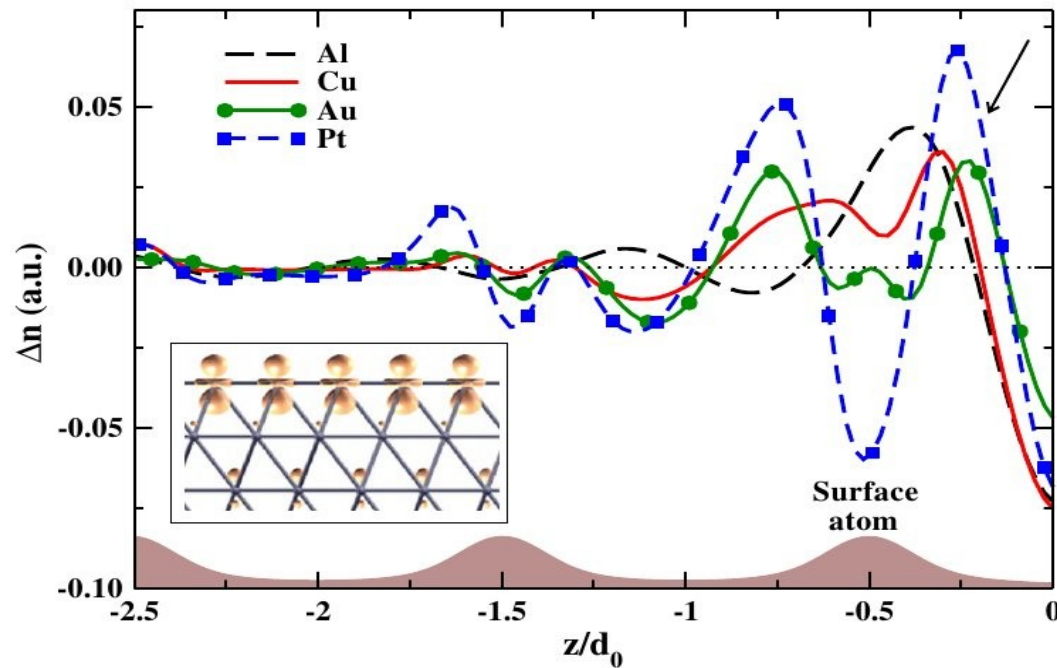
were fixed from the infinite-barrier model



The Q2D-GGA functional

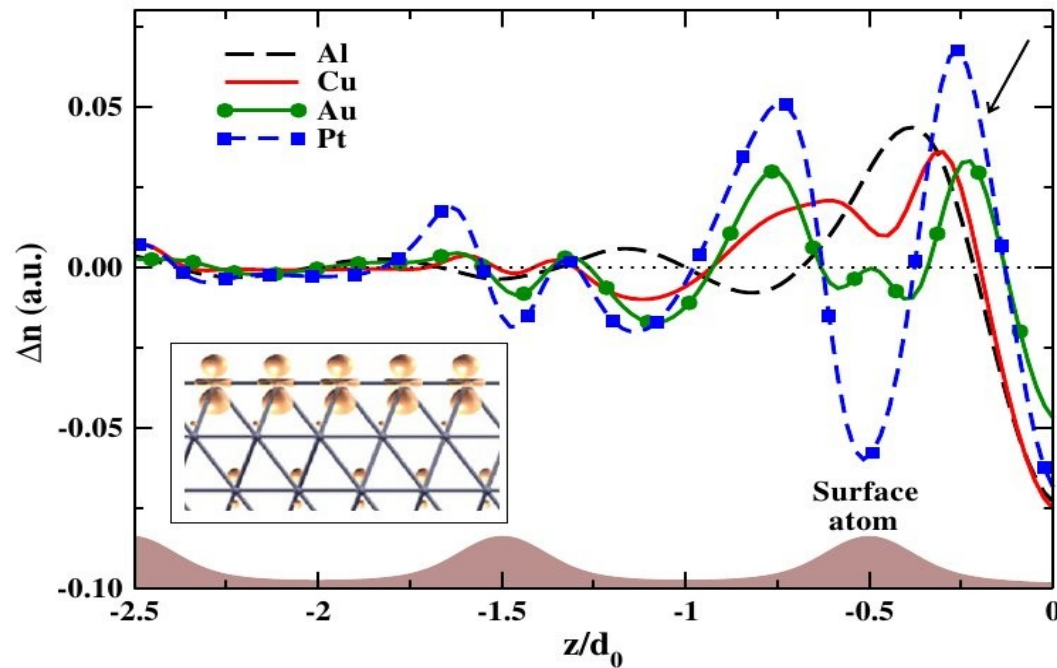
- recovers the correct second-order gradient expansion in the slowly-varying density limit
- satisfies the correct 2D limits in the rapidly varying-density limit
- is close to PBEsol for bulk solids ( $s < 1$ )

# Quasi-2D behavior at metal surfaces

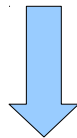


The surface of transition metals shows 2D localization effects due to the degeneracy-splitting of the  $d$ -orbitals. No such effect is present in simple metals

# Quasi-2D behavior at metal surfaces

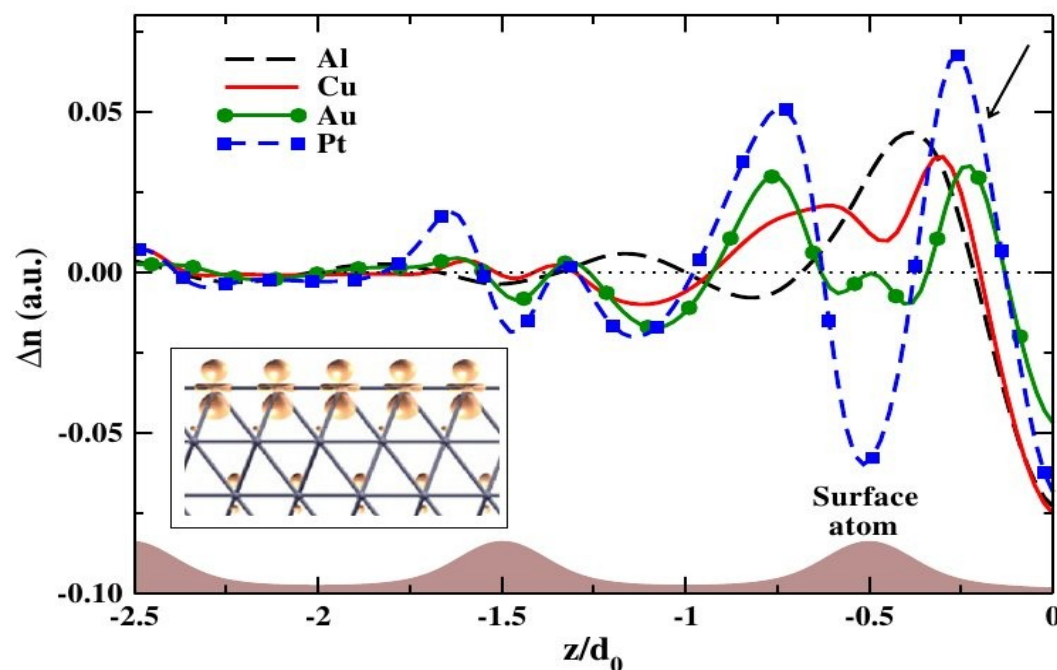


The surface of transition metals shows 2D localization effects due to the degeneracy-splitting of the  $d$ -orbitals. No such effect is present in simple metals

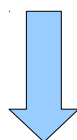


The correct description of the surface-energy of transition metals requires a balanced description of bulk and Q2D regions

# Quasi-2D behavior at metal surfaces



The surface of transition metals shows 2D localization effects due to the degeneracy-splitting of the *d*-orbitals. No such effect is present in simple metals



The correct description of the surface-energy of transition metals requires a balanced description of bulk and Q2D regions

**The Q2D-GGA functional is the best for lattice constants and surface energies**

	LDA	PBE	PBEsol	Q2D-GGA	Exp
Lattice constant [Å]					
Al	3.95	4.04	<b>4.02</b>	3.95	4.02
Cu	3.52	<b>3.63</b>	3.56	3.53	3.60
Rh	3.78	3.86	3.81	<b>3.79</b>	3.79
Au	4.03	4.18	4.10	<b>4.07</b>	4.07
Pt	<b>3.92</b>	4.00	3.95	3.93	3.92
Pd	<b>3.88</b>	3.98	3.92	3.89	3.88
Ti	4.00	<b>4.11</b>	4.06	4.02	4.10
ME	-0.04	0.06	<b>0.01</b>	-0.03	
MAE	0.04	0.06	<b>0.03</b>	<b>0.03</b>	
Surface Energy [J/m <sup>2</sup> ]					
Al	<b>1.10</b>	0.81	0.95	1.25	1.14
Cu	1.94	1.41	<b>1.77</b>	2.06	1.83
Rh	2.50	2.02	2.42	<b>2.85</b>	2.70
Au	1.27	0.73	1.02	<b>1.50</b>	1.50
Pt	2.07	1.56	1.91	<b>2.35</b>	2.49
Pd	1.83	1.27	1.63	<b>2.02</b>	2.00
Ti	2.12	1.85	2.03	<b>2.40</b>	2.47
ME	-0.19	-0.64	-0.34	<b>0.04</b>	
MAE	0.22	0.64	0.34	<b>0.10</b>	



## INTRODUCTION

- Semilocal exchange-correlation functionals
- The family of PBE-like XC functionals

## GGA functionals

- PBEint
- zPBEint
- APBE
- Q2D-GGA

## Meta-GGA functionals

- TPSSloc



# Tail behavior of the PBE correlation



In the rapidly-varying density limit ( $t \rightarrow \infty$ ) the PBE correlation functional shows a slow decaying behavior depending on the value of  $\beta$

$$\epsilon_c^{PBE} \rightarrow \frac{Q}{\beta^2} \frac{1}{t^4} + O\left(\frac{1}{t^6}\right) \text{ with } Q = \gamma^3 \phi^3 \left[ e^{\epsilon_c^{LDA}/(\gamma \phi^3)} - 1 \right]^3 e^{-2\epsilon_c^{LDA}/(\gamma \phi^3)} < 0$$

However,  $\beta$  is fixed by imposing conditions on the slowly-varying density limit and there is no reason why it should control the behavior at  $t \rightarrow \infty$

# Tail behavior of the PBE correlation

In the rapidly-varying density limit ( $t \rightarrow \infty$ ) the PBE correlation functional shows a slow decaying behavior depending on the value of  $\beta$

$$\epsilon_c^{PBE} \rightarrow \frac{Q}{\beta^2} \frac{1}{t^4} + O\left(\frac{1}{t^6}\right) \text{ with } Q = \gamma^3 \phi^3 \left[ e^{\epsilon_c^{LDA}/(\gamma \phi^3)} - 1 \right]^3 e^{-2\epsilon_c^{LDA}/(\gamma \phi^3)} < 0$$

However,  $\beta$  is fixed by imposing conditions on the slowly-varying density limit and there is no reason why it should control the behavior at  $t \rightarrow \infty$

This situation is corrected by considering

$$\beta(r_s, t) = \beta_0 + at^2 f(r_s) \longrightarrow$$

so that

$$\epsilon_c^{PBEloc} \rightarrow \frac{Q}{[af(r_s)]^2} \frac{1}{t^8} + O\left(\frac{1}{t^{10}}\right)$$

Now,  $\beta_0$  only determines the behavior in the slowly-varying density limit and we can set

$$\beta_0 = \frac{3\mu_x^{GE2}}{\pi^2} \approx 0.0375$$

The function  $f(r_s)$  is fixed by imposing a proper behavior of the functional under uniform scaling to the low- and high-density limit

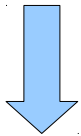
$$f(r_s) = 1 - e^{-r_s^2}$$

The parameter  $a=0.08$  is fixed by fitting to jellium surface correlation energies

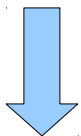
# Localization of the PBE correlation

In a neutral spherical atom

$r_s$  and  $t \gg 1$  in the tail  
 $r_s \rightarrow 0$  and  $t \sim Z$  in the core



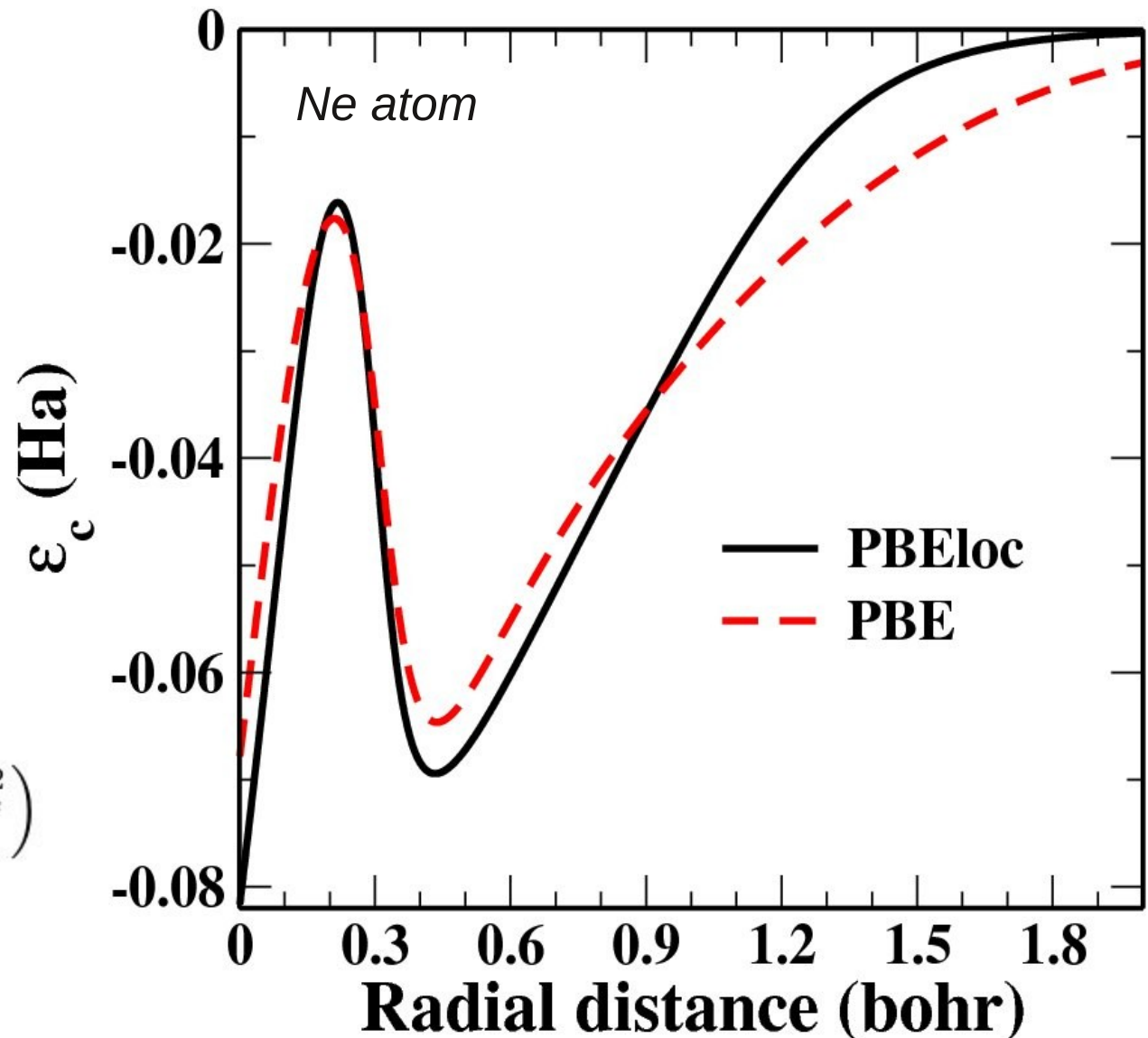
$\beta \gg \beta_0$  in the tail  
 $\beta \rightarrow \beta_0$  in the core



The choice

$$\beta(r_s, t) = \beta_0 + at^2 (1 - e^{-r_s^2})$$

corresponds to a localization of the PBE correlation



# The TPSSloc correlation functional

The PBEloc correlation can be used to construct a meta-GGA correlation functional with increased localization

Following the TPPS construction:

$$E_c^{TPSSloc} = \int \rho \tilde{\epsilon}_c \left[ 1 + d \tilde{\epsilon}_c z^3 \right] d\mathbf{r} \quad z = \frac{\tau_W}{\tau}$$

$$\tilde{\epsilon}_c = \epsilon_c^{PBEloc} \left[ 1 + C(\zeta, \eta) z^2 \right] - [1 + C(\zeta, \eta)] z^2 \sum_{\sigma} \frac{\rho_{\sigma}}{\rho} \bar{\epsilon}_{\sigma}$$

$$\bar{\epsilon}_{\sigma} = \max \left[ \epsilon_c^{PBEloc}(\rho_{\sigma}, 0, \nabla \rho_{\sigma}, 0); \epsilon_c^{PBEloc}(\rho_{\uparrow}, \rho_{\downarrow}, \nabla \rho_{\uparrow}, \nabla \rho_{\downarrow}) \right]$$

$$C(\zeta, \eta) = \frac{C(0, 0) + 0.87\zeta^2 + 0.50\zeta^4 + 2.26\zeta^6}{[1 + \zeta^2 [(1 + \eta)^{-4/3} + (1 - \eta)^{-4/3}] / 2]^4} \quad \eta = \frac{|\nabla \zeta|}{2(3\pi^2)^{1/3} \rho^{1/3}}$$

The parameters

$d = 4.5$

$C(0, 0) = 0.35$

have been fixed by fitting to jellium surfaces and Hooke's atom

# Assessment of the TPSSloc functional



Test set	(L)HF + LYP	(L)HF + PBE	(L)HF + PBEloc
AE6	38.2 (41.3)	31.9 (35.4)	<b>24.0 (26.7)</b>
BH6	5.3 ( <b>7.2</b> )	5.6 (7.8)	<b>4.4</b> (7.4)
K9	6.0 (7.0)	5.7 (7.4)	<b>4.7 (6.9)</b>
HB6	2.3 (1.7)	<b>1.5 (1.0)</b>	1.7 (1.2)

Test set	(L)HF + TPSS	(L)HF + revTPSS	(L)HF + TPSSloc
AE6	29.1 (31.4)	30.0 (31.0)	<b>25.5 (27.4)</b>
BH6	4.7 (6.7)	5.1 (6.9)	<b>3.9 (6.6)</b>
K9	5.6 (6.7)	6.1 (6.8)	<b>4.3 (6.4)</b>
HB6	<b>1.4 (0.9)</b>	1.5 (1.0)	1.6 (1.1)

## Exact exchange + cTPSSloc

The localization procedure strongly improves the compatibility of the semilocal functional with exact exchange

# Assessment of the TPSSloc functional



Test set	(L)HF + LYP	(L)HF + PBE	(L)HF + PBEloc
AE6	38.2 (41.3)	31.9 (35.4)	<b>24.0 (26.7)</b>
BH6	5.3 ( <b>7.2</b> )	5.6 (7.8)	<b>4.4</b> (7.4)
K9	6.0 (7.0)	5.7 (7.4)	<b>4.7 (6.9)</b>
HB6	2.3 (1.7)	<b>1.5 (1.0)</b>	1.7 (1.2)

## Exact exchange + cTPSSloc

The localization procedure strongly improves the compatibility of the semilocal functional with exact exchange

Test set	(L)HF + TPSS	(L)HF + revTPSS	(L)HF + TPSSloc
AE6	29.1 (31.4)	30.0 (31.0)	<b>25.5 (27.4)</b>
BH6	4.7 (6.7)	5.1 (6.9)	<b>3.9 (6.6)</b>
K9	5.6 (6.7)	6.1 (6.8)	<b>4.3 (6.4)</b>
HB6	<b>1.4 (0.9)</b>	1.5 (1.0)	1.6 (1.1)

## xrevTPSS + cTPSSloc

The TPSSloc correlation functional works very well in combination with the revTPSS exchange, yielding results even better than the original revTPSS functional

Test set	TPSS	revTPSS	TPSSloc
AE6	5.4	6.6	<b>3.9</b>
BH6	8.3	<b>7.4</b>	8.6
HB6	<b>0.6</b>	<b>0.6</b>	<b>0.6</b>
K9	7.0	7.2	<b>6.5</b>
TM10	10.7	11.1	<b>10.5</b>
MGBL19	6.9	7.4	<b>6.8</b>
IP13	3.1	<b>2.9</b>	3.0
PA12	4.7	4.8	<b>3.8</b>
OMRE	8.0	10.2	<b>7.9</b>



# Assessment of the TPSSloc functional

Test set	(L)HF + LYP	(L)HF + PBE	(L)HF + PBEloc
AE6	38.2 (41.3)	31.9 (35.4)	<b>24.0 (26.7)</b>
BH6	5.3 ( <b>7.2</b> )	5.6 (7.8)	<b>4.4</b> (7.4)
K9	6.0 (7.0)	5.7 (7.4)	<b>4.7 (6.9)</b>
HB6	2.3 (1.7)	<b>1.5 (1.0)</b>	1.7 (1.2)

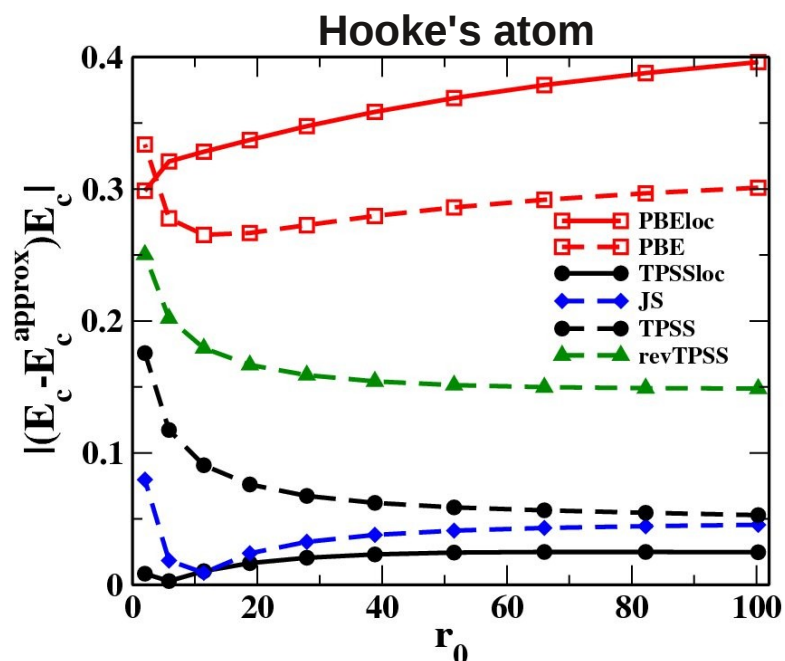
## Exact exchange + cTPSSloc

The localization procedure strongly improves the compatibility of the semilocal functional with exact exchange

Test set	(L)HF + TPSS	(L)HF + revTPSS	(L)HF + TPSSloc
AE6	29.1 (31.4)	30.0 (31.0)	<b>25.5 (27.4)</b>
BH6	4.7 (6.7)	5.1 (6.9)	<b>3.9 (6.6)</b>
K9	5.6 (6.7)	6.1 (6.8)	<b>4.3 (6.4)</b>
HB6	<b>1.4 (0.9)</b>	1.5 (1.0)	1.6 (1.1)

## xrevTPSS + cTPSSloc

The TPSSloc correlation functional works very well in combination with the revTPSS exchange, yielding results even better than the original revTPSS functional



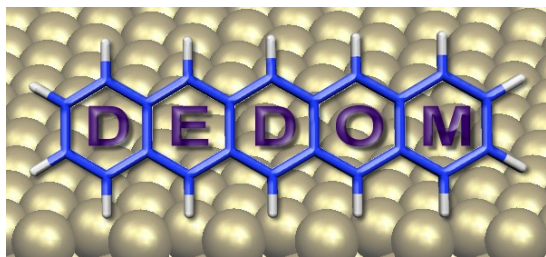
Test set	TPSS	revTPSS	TPSSloc
AE6	5.4	6.6	<b>3.9</b>
BH6	8.3	<b>7.4</b>	8.6
HB6	<b>0.6</b>	<b>0.6</b>	<b>0.6</b>
K9	7.0	7.2	<b>6.5</b>
TM10	10.7	11.1	<b>10.5</b>
MGBL19	6.9	7.4	<b>6.8</b>
IP13	3.1	<b>2.9</b>	3.0
PA12	4.7	4.8	<b>3.8</b>
OMRE	8.0	10.2	<b>7.9</b>

- GGA functionals provide the best compromise between accuracy and computational cost, for large applications of DFT
- No GGA can provide good accuracy for any problem, because of the limitations of the gradient-dependent semilocal approximation
- GGA functionals can be of great utility in DFT if the proper approximation is used for each specific application
- We developed several non-empirical GGA functionals for various problems:
  - **PBEint, zPBEint** Surfaces, interfaces, clusters
  - **APBE** Molecules, organic chemistry
  - **Q2D-GGA** Solid-state, transition-metal surfaces, 2D problems
- The development of improved GGA functionals is fundamental also for the construction of better functionals on the higher rungs of the DFT Jacob's ladder
- The use of a localization technique for the PBE correlation allows to construct the TPSSloc meta-GGA correlation functional with significant higher compatibility with exact exchange



Thanks to:

- Dr. L.A. Constantin
- Dr. F. Della Sala
- NNL theory group



Development of Density-Functional  
Theory Methods for  
Organic-Metal interaction (2008-2013)

